HEDL-SA-1750

CONF-790615--20

MASTER

# THE FATIGUE-CRACK PROPAGATION RESPONSE OF TWO NICKEL-BASE ALLOYS IN A LIQUID SODIUM ENVIRONMENT

William J. Mills,
Senior Engineer

and

Lee A. James,
Fellow Engineer, Member ASME

January 23, 1979

To be Presented at the
ASME Pressure Vessel and Piping Conference,

June 25-29, 1979, San Francisco

**HANFORD ENGINEERING DEVELOPMENT LABORATORY**
**Operated by Westinghouse Hanford Company, a subsidiary of Westinghouse Electric Corporation, under the Department of Energy Contract No. EY-76-C-14-2170**

## DISCLAIMER

# THE FATIGUE-CRACK PROPAGATION RESPONSE OF TWO NICKEL-BASE ALLOYS IN A LIQUID SODIUM ENVIRONMENT

William J. Mills and Lee A. James

## ABSTRACT

*The elevated temperature fatigue-crack propagation response of Inconel 600 and Inconel 718 was characterized within a linear-elastic fracture mechanics framework in air and low-oxygen liquid sodium environments. The crack growth rates of both nickel-base alloys tested in liquid sodium were found to be considerably lower than those obtained in air. This enhanced fatigue resistance in sodium was attributed to the very low oxygen content in the inert sodium environment.*

*Electron fractographic examination of the Inconel 600 and Inconel 718 fatigue fracture surfaces revealed that operative crack growth mechanisms were dependent on the prevailing stress intensity level. Under low growth rate conditions, Inconel 600 and Inconel 718 fracture surfaces exhibited a faceted, crystallographic morphology in both air and sodium environments. In the higher growth rate regime, fatigue striations were observed; however, striations formed in sodium were rather ill-defined. These indistinct striations were attributed to the absence of oxygen in the liquid sodium environment. Striation spacing measurements were found to be in excellent agreement with macroscopic growth rates in both environments.*

## INTRODUCTION

Nickel-base alloys are being used, or being considered for use, in liquid-metal fast-breeder reactor applications where elevated temperature strength, creep behavior, and corrosion resistance are important considerations. More specifically, two nickel-base alloys-Inconel 600,* a solid-solution-strengthened nickel-base alloy, and Inconel 718,** a precipitation hardenable nickel-base superalloy - are being utilized for several high temperature structural components in breeder reactor designs. Such components are often subjected to cyclic stresses during service; hence, fatigue-crack propagation (FCP) could occur should defects be present in the appropriate size, shape and orientation. Linear-elastic fracture mechanics techniques have proven to be very useful for predicting the in-service subcritical extension of such flaws, either hypothetical defects or actual crack-like defects, but their usage requires a complete understanding of the material's FCP response under the appropriate service conditions (temperature, cyclic frequency, stress ratio, heat-treatment, thermal aging and environment). The effect of many of these parameters on the cyclic response of Inconel 718 has been characterized previously, including the effect of: temperature,[1-5] cyclic frequency and waveform,[5-7] cyclic stress ratio,[4,8-10] heat treatment,[4,11-16] and heat-to-heat variations.[14,16] In addition, the influence of temperature[1,17] cyclic stress ratio,[17] and thermal aging[17] on the crack growth behavior of Inconel 600 has also been

---

* Inconel 600 is a registered trademark of the International Nickel Company. The general specifications covering the material may be found in ASTM specification B-168 for plate, sheet, and strip.

** Inconel 718 is a registered trademark of the International Nickel Company. The general specifications for this material may be found in ASTM Specification A-637 Grade 718 for bar and forgings, and in SAE Specifications AMS-5596 and AMS 5597 for sheet, strip and plate.

determined. The majority of these studies, however, have been conducted in an air environment. On the other hand, since many fast-breeder reactor components operate in a liquid sodium environment, rather than an air environment, the current study was undertaken to characterize the effect of liquid sodium on the fatigue-crack growth response of Inconel 600 and Inconel 718 within a linear-elastic fracture mechanics framework at a typical breeder reactor operation temperature of 800°F (427°C). In addition, the fatigue fracture surface micromorphology of the two nickel-base alloys was examined in order to improve the basic understanding of operative FCP processes in a sodium environment.

The environment can have a profound effect upon the crack growth behavior of structural components, and this appears to be especially true at elevated temperatures. To-date, several investigations have been performed in order to characterize the environmental influence of liquid sodium on FCP rates for a number of reactor materials including: Types 304[18] and 316[19-21] austenitic stainless steels, and a pressure vessel steel A-387 Grade D.[22] The results of these studies indicate that under low stress intensity range ($\Delta K$) conditions where the environment is expected to be most influential, crack growth rates in liquid sodium were considerably lower (by approximately a factor of 5 to 10) than FCP rates in air. In the higher $\Delta K$ regime, the effect of environment on fatigue behavior was less pronounced as the cyclic growth rates in sodium tended to approach those in elevated temperature air.[18,20,21] James and Knecht[18] also reported that crack growth rates in liquid sodium and in vacuum were identical at both 800 and 1000°F (427 and 538°C), thereby suggesting that the sodium environment is approximately as inert as a vacuum.

## EXPERIMENTAL PROCEDURE

### Material

The 1-inch (25.4 mm) thick plate of Inconel 600 used in this study was obtained from heat NX-9929-1A produced by the Huntington Alloy Products Division of the International Nickel Company using an air melt process. This material was tested in the as-received (solution annealed) condition:

- Annealed 45 minutes at 1585°F (863°C)
- Air cooled.

The Inconel 718 used during the current investigation was furnished in the form of a 0.5-inch (12.7 mm) thick plate from heat 52C9EK which was also produced by the Huntington Products Division of the International Nickel Company using a vacuum-induction-melted, electro-flux-remelted process (VIM-EFR). It was tested in the precipitation-hardened condition:

- Annealed 1 hour at 1750°F (954°C), and air cooled
- Aged 8 hours at 1325°F (718°C)
- Furnace-cooled to 1150°F (621°C)
- Held at 1150°F (621°C) for a total aging time of 18 hours
- Air cooled.

The chemical compositions and mechanical properties for these two nickel-base alloys are given in Tables I and II, respectively.

### Crack Growth Testing in a Liquid Sodium Environment

In-sodium fatigue testing was performed in a specially-designed chamber (consult Reference 18 for a complete description of the sodium testing apparatus) that allowed a continuous flow of sodium around the fatigue specimen. Sodium entered the test chamber through the bottom, flowed around the specimen, and then exited through the top (see Figure 1). The temperature within this chamber was controlled to within $\pm 2$°F ($\pm 1$°C). Impurity levels within the sodium (see Table III) were controlled by a cold trap.

ASTM Compact Specimens [E647-78T] were cyclically loaded inside the sodium chamber using a feedback-controlled electro-hydraulic test system operated in load control. A schematic diagram of this test system is given in Figure 1 with the actual loading system shown in Figures 2. At the completion of a test, an argon purge was used to force the sodium out of the chamber. Removal of the tested specimen and insertion of a new specimen was accomplished by opening the sodium chamber inside a specially-constructed glovebox such that the contamination of the specimens and chamber was minimized.

To measure an increment of crack extension associated with a given number of cycles, a fracture face marking technique was utilized.[18] With this technique the maximum cyclic load was held constant throughout the test while the minimum cyclic load was varied periodically. Each change in minimum cyclic load (and stress ratio) was accompanied by a mark or change in texture on the fatigue fracture surface. Typical macroscopic growth bands on the fracture face are shown in Figure 3. Such contours were then measured from the fracture surface after the test was completed. Specimens were not cycled to failure since tests were terminated after a predetermined loading program was run. Following each test, the specimen was removed from the chamber, cleaned of sodium and broken open to reveal the fracture face markings. The crack length (a) along a given contour was determined by averaging the crack length at the 1/4-, 1/2- and 3/4- thickness planes. The crack growth rate (da/dN) was calculated by dividing each increment between contours ($\Delta a$) by the number of cycles providing that increment ($\Delta N$). The stress intensity factor (K) was based on the average crack length for each macroband increment ($a + \Delta a/2$); calculations were made using the standard K-solution given in E647-78T.

As mentioned previously, the fracture surface contours on specimens tested in sodium were produced by changing the stress ratio ($R = K_{min}/K_{max}$). Consequently, an "effective" stress intensity factor[23] ($K_{eff}$) was used to characterize the fatigue behavior since it was shown that this parameter provides an excellent correlation of crack growth rates over a wide range of stress ratios.[24,25]. The effective stress intensity factor is defined as

$$K_{eff} = K_{max} [1 - R]^m$$

where the exponent "m" is dependent on material and temperature, but apparently it is not dependent on environment.[24] Values of "m" for Inconel 600 and Inconel 718 at 427°C was found to be 0.4[17] and 0.5,[4,24] respectively. The fatigue results obtained during this study are therefore displayed as plots of log (da/dN) vs log ($K_{eff}$).

Fractographic Techniques

To characterize the fatigue-crack growth mechanisms in liquid sodium, standard two-stage carbon replicas shadowed parallel to the crack growth direction were made from the fracture surfaces. Care was taken in cutting the replicas into strips along the fracture markings in an effort to relate features observed on the fracture face to a corresponding growth rate and $K_{eff}$ level. Electron microscopic examination of the replicas was performed on a Phillips electron microscope operated at an accelerating potential of 60 kV.

## PRESENTATION AND DISCUSSION OF RESULTS

### Fatigue Crack Propagation in Liquid Sodium

Fatigue testing of Inconel 600 and Inconel 718 in a liquid sodium environment was performed during the current investigation at a test temperature of 800°F (427°C).

The results of these tests were compared with FCP data generated previously in an air environment for these same heats of Inconel 600[1,17] and Inconel 718[4,14] (see Figures 4-6). Comparison of the fatigue behavior of Inconel 600 specimens tested in air and sodium (Figure 4) reveals that crack growth rates in sodium were approximately a factor of 2 to 4 times lower than those obtained in air under low $K_{eff}$ conditions (below 25 ksi $\sqrt{in}$). At higher stress intensity levels, the effect of environment was less pronounced as FCP rates in sodium were only slightly lower than those in air. This phenomenon is attributed to the fact that new crack surfaces are being created at a faster rate than the environmental (i.e., air) attack at high $K_{eff}$ levels. Finally, Figure 5 reveals that the elevated temperature FCP behavior in sodium was almost identical to the room temperature crack growth response in air, thereby suggesting that the thermally-activated increase in FCP rates observed in air is in all likelihood due to an environmental attack rather than a creep-fatigue interaction. This suggestion has been made previously[2,18, 26,27] when comparing FCP rates in elevated temperature "inert" environments (vacuum, liquid sodium, inert gasses) and room temperature air.

The Inconel 718 fatigue results obtained in low-oxygen sodium and air environments at 800°F (427°C) are shown in Figure 6. This figure reveals that the fatigue crack growth rate in a liquid sodium environment was approximately an order of magnitude lower than in an air environment, which is consistent with the overall trends observed in Inconel 600 and the various steel alloys[18-22].

The data shown in Figure 6 was generated using a cyclic frequency of 400 cpm, with the exception of a limited amount of data at 40 cpm in the sodium environment. This limited data suggests that there was no observable effect of frequency over this very narrow frequency range. It should be noted, however, that there is only a very small frequency effect over the same frequency range in an air environment at 800°F (427°C)[4]. Minor frequency effects were suggested

when comparing the FCP results for Type 316 tested at 0.33-0.5 cpm in liquid sodium[21] with those for Type 304 stainless steel tested in sodium at 180-400 cpm in Reference 18.

The data from the Inconel 718 specimen tested in sodium represents a relatively narrow range of values of $K_{eff}$. This is because the crack grew at a rate lower than expected, and hence the growth increments upon which the crack growth rates were based were smaller than optimum. Therefore, although the data points for Specimen 160 (Figure 6) do not exhibit excessive scatter and are considered valid, some minor errors may have been introduced due to the relatively small growth increments.

In summary, the decrease in crack growth rates in liquid sodium exhibited by Inconel 600 and Inconel 718 is in quantitative agreement with previous observations on the effect of a liquid sodium environment on FCP behavior in austenitic stainless steels[18-21] and a ferritic steel[22]. Liquid sodium is obviously an inert environment, insofar as fatigue-crack growth is concerned, and this beneficial effect is believed to be associated with a very low oxygen level in the liquid sodium[18].

## FRACTURE SURFACE MICROMORPHOLOGY

The fracture surface micromorphologies of Inconel 600 and Inconel 718 fatigue tested at 800°F (427°C) in air and liquid sodium were examined to characterize operative crack growth mechanisms in both environments. The fracture surface markings for Inconel 600 tested in air consisted of three FCP mechanisms with the operative crack growth mechanism depending on the prevailing stress intensity factor. Under the highest stress intensity factor conditions, the fatigue fracture surface exhibited a highly striated appearance (Figure 7a) coupled with a few microvoids as shown in Figure 7b. At intermediate $K_{eff}$

levels [22 to 40 ksi $\sqrt{in}$ (24-44 MPa $\sqrt{m}$)], crack propagation also occurred by fatigue striation formation (Figure 7c); however, no evidence of dimple rupture was observed. The microscopic FCP rates determined from striation spacing measurements are compared with macroscopic growth rates in Figure 8. These results reveal that the microscopic and macroscopic FCP rates for Inconel 600 in air were in excellent agreement.

Under low stress intensity conditions, the fatigue fracture surface exhibited a faceted appearance (Figure 9a) indicative of crystallographic cracking along active slip planes. In addition, rather indistinct lines were often observed superimposed on the facets (Figures 9a and 9b); however, the spacing of these lines was almost an order of magnitude larger than the macroscopic FCP rates, thereby suggesting that these facture markings represent slip offset rather than fatigue striations.

The fracture surface markings observed in Inconel 600 tested in sodium were found to be rather similar to those observed in air. At high stress intensity levels, fatigue striations were occasionally observed on the fracture surface (Figures 10a and 10b); however, the striations formed in sodium were poorly defined in comparison to those formed in air (Figure 7). Nevertheless, the spacings of these indistinct fatigue striations were found to be in excellent agreement with the macroscopic FCP rates in sodium as illustrated in Figure 8.

The appearance of relatively few indistinct striations on the Inconel 600 fatigue fracture surfaces tested in sodium is comparable to the ill defined, flattened striations[28,29] reported in other materials fatigue tested in vacuum. This overall lack of well defined striations in vacuum was attributed to more efficient slip reversal in the crack tip region due to the absence of an oxide film on the newly formed crack surfaces[29-34]. This resulted in the formation of very

shallow, ill defined striations that were visible only under optimum conditions. In a similar fashion, the "inert" liquid sodium environment prevented oxygen from reaching the crack tip region, thereby eliminating the formation of an oxide layer on the newly exposed crack surfaces. This absence of an oxide film enhanced reversed slip ahead of the crack tip which resulted in the shallow, indistinct striations (Figures 10a and 10b) observed on the Inconel 600 fatigue fracture surface under high crack growth rate conditions.

The fracture surface of the Inconel 600 tested in sodium at low $K_{eff}$ levels took on a highly faceted or cleavage-like morphology (Figure 10c) comparable to the crystallographic cracking reported by Scarlin[29] in another nickel-base alloy cyclically loaded in vacuum. It should also be noted that this faceted appearance coupled with the periodic fine lines superimposed on the facets, as illustrated in Figure 10c, was very similar to the fracture surface morphology observed in air (Figure 9). The spacings of these periodic fracture markings formed in liquid sodium were found to be consistently greater than the macroscopic FCP rate, here again indicating that these slip offsets were of a non-cyclic nature.

The fatigue fracture surfaces of Inconel 718 cyclically loaded at 800°F (427°C) in air and liquid sodium environments were also found to be very similar to each other under low $K_{eff}$ conditions. As shown in Figures 11 and 12, the faceted growth behavior with distinctive parallel fracture markings often superimposed on the facets was dominant in both air and liquid sodium, thereby suggesting that essentially the same FCP mechanism operates in both environments in the low stress intensity regime. The spacing of these parallel markings (Figures 11b, 11c, 12a and 12b),

approximately 500Å, was an order of magnitude greater than macroscopic crack growth rates which indicates that these non-cyclic fracture markings represent slip offsets produced by the severe stresses present in the wake of the crack front. Finally, it is interesting to note in Figure 11d that two sets of slip offsets, associated with slip on multiple slip systems, have intersected each other.

Under intermediate and high FCP rate levels in an air environment, the Inconel 718 exhibited striation and dimple rupture mechanisms as reported in Reference 14 for the same heat of material studied in the current investigation. Unfortunately, the fatigue fracture mechanisms operating in liquid sodium under relatively high growth rate conditions were not determined since Specimen 160 was not tested in this regime (see Figure 6).

## CONCLUSIONS

The fatigue crack growth responses of Inconel 600 and Inconel 718 were examined at 800°F (427°C) in air and liquid sodium environments and the following conclusions were drawn:

1. The elevated temperature fatigue crack growth rates of Inconel 600 and Inconel 718 in low-oxygen liquid sodium were considerably lower than those in air, particularly in the lower FCP rate regime. This improved cyclic response in liquid sodium is believed to be associated with very low oxygen levels in the inert sodium environment.

2. Under high crack growth rates conditions, the Inconel 600 fracture surfaces exhibited evidence of fatigue striations in both environments; however, striations formed in sodium were rather ill defined. These shallow, indistinct striations formed in the low-oxygen sodium environment were attributed to more

enhanced slip reversals due to the absence of an oxide film on the newly formed crack surfaces.

3. The Inconel 600 microscopic FCP rates, striation spacings, were found to be in excellent agreement with macroscopic crack growth rates in both air and liquid sodium environments.

4. In the low fatigue crack growth rate regime, Inconel 600 and Inconel 718 fatigue fracture surfaces exhibited crystallographic cracking along preferred crystal planes in both air and liquid sodium environments.

## ACKNOWLEDGEMENTS

This paper is based on work performed under U.S. Department of Energy (DOE) contract EY-76-C-14-2170 with the Westinghouse Hanford Company, a subsidiary of Westinghouse Electric Corporation.

The efforts of D. J. Criswell in helping to conduct these tests are greatly appreciated. In addition, the authors want to acknowledge B. Mastel who helped perform the electron microscopy.

REFERENCES

(1) James, L. A., "The Effect of Temperature Upon the Fatigue-Crack Growth Behavior of Two Nickel-Base Alloys," Journal of Engineering Materials and Technology, Trans. ASME, Series H, Vol. 95, No. 4, Oct. 1973, pp. 254-256.

(2) Speidel, M. O., "Fatigue-Crack Growth at High Temperatures," High Temperature Materials in Gas Turbines, Elsevier Publishing Co., Amsterdam, 1974, pp. 207-251.

(3) Tobler, R. L., "Low Temperature Effects on the Fracture Behavior of a Nickel-Base Superalloy," Cryogenics, Vol. 16, No. 1, Nov. 1976, pp. 669-674.

(4) James, L. A., "Fatigue-Crack Propagation Behavior of Inconel 718," Report HEDL-TME 75-80, Westinghouse Hanford Co., Sept. 1975.

(5) Popp, H. G., and Coles, A., "Subcritical Crack Growth Criteria for Inconel 718 at Elevated Temperatures," Proceedings Air Force Conference on Fatigue and Fracture of Aircraft Structures and Materials, H. A. Woods, et al. (Eds.) pp. 71-96, Report AFFDL TR 70-144, Air Force Flight Dynamics Laboratory, September 1970.

(6) Shahinian, P. and Sadananda, K., "Crack Growth Behavior Under Creep-Fatigue Conditions in Alloy 718," 1976 ASME-MPC Symposium on Creep-Fatigue Interactions, Series MPC-3, pp. 365-390, American Society of Mechanical Engineers, New York, 1976.

(7) Clavel, M. and Pineau, A., "Frequency and Wave-Form Effects on the Fatigue Crack Growth Behavior of Alloy 718 at 298K and 823K," Metallurgical Transactions, Vol. 9A, 1978, pp. 471-480.

(8) Coles, A., Johnson, R. E., and Popp, H. G., "Utility of Surface-Flawed Tensile Bars in Cyclic Life Studies," Journal of Engineering Materials and Technology, Vol. 98, pp. 305-315, 1976.

(9) James, L. A., "The Effect of Stress Ratio Upon the Elevated Temperature Fatigue-Crack Growth Behavior of Several Reactor Structural Materials," Report HEDL-TME 75-20, Westinghouse Hanford Company, 1975.

(10) James, L. A., "Stress Ratio Effects Upon the Fatigue-Crack Growth Behavior of Inconel 718," in Report ORNL-5287, Oak Ridge National Laboratory pp. 370-384, 1977.

(11) Smith, H. H., and Michel, D. J., "Fatigue Crack Propagation in Alloy 718: Effect of Heat Treatment on Microstructure and Fatigue Behavior," in Report ORNL-5255, Oak Ridge National Laboratory, Mar. 1977, pp. 270-277.

(12) Smith, H. H. and Michel, D. J., "Fatigue Crack Propagation in Alloy 718: Effect of Heat Treatment on Microstructure and Fatigue Performance at 427°C," in Report ONRL-5349, Oak Ridge National Laboratory, Dec. 1977, pp. 185-190.

(13) Smith, H. H. and Michel, D. J., "Fatigue Crack Propagation and Deformation Mode in Alloy 718 at Elevated Temperatures," Ductility and Toughness Considerations in Elevated Temperature Service, ASME, 1978, pp. 225-246.

(14) Mills, W. J., and James, L. A., "Effect of Heat-Treatment on Elevated Temperature Fatigue-Crack Growth Behavior of Two Heats of Alloy 718," ASME Paper 78-WA/PVP-3, 1978.

(15) James, L. A., "Fatigue-Crack Growth in Inconel 718 Weldments at Elevated Temperatures," Welding Journal Reserach Supplement, Vol. 57, No. 1, pp. 17s-23s, 1978.

(16) Logsdon, W. A., Kossowsky, R., and Wells, J. M., "The Influence of Processing and Heat Treatment on the Cryogenic Mechanics Properties of Inconel 718," Report 77-9E7-CRYMT-P2, Westinghouse Reserach Laboratories, March 1977.

(17) James, L. A., "Fatigue-Crack Propagation Behavior of Inconel 600," International Journal of Pressure Vessel and Piping, Vol. 5, 1977, pp. 241-259.

(18) James, L. A. and Knecht, R. L., "Fatigue Crack Propagation Behavior of Type 304 Stainless Steel in a Liquid Sodium Environment," Metallurgical Transactions, Vol. 6A, 1975, pp. 109-116.

(19) Marshall, P., "The Fatigue Behavior of Annealed AISI 316 Stainless Steel in Air and High Temperature Sodium: Review and Preliminary Results," Report RD/B/N3236, Central Electricity Generating Board, 1974.

(20) Priddle, E. K. and Wiltshire, C., "The Measurement of Fatigue Crack Propagation in Specimens Immersed in Liquid Sodium at Elevated Temperatures: Technique and Preliminary Results," International Journal of Fracture, Vol. 11, 1975, pp. 697-700.

(21) Copeland, J. F. and Yuen, J. L., "Fatigue Crack Growth Properties of Type-316 Plate and 16-8-2 Stainless Steel Welds in Air and High Carbon Liquid Sodium," Report GEFR-00303, General Electric Co., Sunnyvale, CA, 1977.

(22) James, L. A., "Effect of a Liquid Sodium Environment Upon Fatigue-Crack Growth in a Pressure Vessel Steel," Scripta Metallurgia, Vol. 10, 1976, pp. 1039-1042.

(23) Walker, K., "The Effect of Stress Ratio During Crack Propagation and Fatigue for 2024-T3 and 7075-T6 Aluminum," Effects of Environment and Complex Load History on Fatigue Life, ASTM STP 462, American Society for Testing and Materials, 1970, pp. 1-14.

(24) James, L. A., "The Effect of Stress Ratio Upon the Elevated Temperature Fatigue-Crack Growth Behavior of Several Reactor Structural Materials," Report HEDL-TME 75-20, Westinghouse Hanford Company, 1975.

(25) James, L. A., "The Effect of Stress Ratio on the Elevated Temperature Fatigue-Crack Propagation of Type 304 Stainless Steel," Nuclear Technology, Vol. 14, No. 2, 1972, pp. 163-170.

(26) James, L. A., "Some Questions Regarding the Interaction of Creep and Fatigue," Journal of Engineering Materials and Technology, Vol. 98, No. 3, 1976, pp. 235-243.

(27) Mahoney, M. W. and Paton, N. E., "The Influence of Gas Environments on Fatigue Crack Growth Rates in Types 316 and 321 Stainless Steel," Nuclear Technology, Vol. 23, No. 3, 1974, pp. 290-297.

(28) Ritter, D. L. and Wei, R. P., "Fractographic Observations of Ti-6-Al-4V Alloy Fatigued in Vacuum," Metallurgical Transactions, Vol. 2, 1971, pp. 3229-3230.

(29) Scarlin, R. B., "Some Effects of Microstructure and Environment on Fatigue Crack Propagation," Fatigue Mechanisms, ASTM STP 675, American Society for Testing and Materials, 1979.

(30) Wanhill, R. J. H., "Fractography of Fatigue Crack Propagation in 2024-T3 and 7075-T6 Aluminum Alloys in Air and Vacuum," Metallurgical Transactions, Vol. 6A, 1975, pp. 1587-1596.

(31) Meyn, D. A., "The Nature of Fatigue-Crack Propagation in Air and Vacuum for 2024 Aluminum," Transactions of the ASM, Vol. 61, 1968, pp. 52-61.

(32) Pelloux, R. M. N., "Crack Extension By Alternating Shear," Engineering Fracture Mechanics, Vol. 1, 1970, pp. 697-204.

(33) Pelloux, R. M. N., "Corrosion-Fatigue Crack Propagation," Fracture, Chapman and Hall, London, 1969, pp. 731-744.

(34) Laird, C. and de la Veaux, R., "Additional Evidence for the Plastic Blunting Process of Fatigue Crack Propagation," Metallurgical Transactions, Vol. 8A, 1977, pp. 657-664.

TABLE I

CHEMICAL COMPOSITION (Percent by Weight

| Material | Producer Heat No. | C | Mn | Fe | S | Si | Cu | Ni | Cr | Al | Ti | Co | Mo | Cb & Ta |
|---|---|---|---|---|---|---|---|---|---|---|---|---|---|---|
| Inconel 600 | Huntington NX-9929-1A | .05 | .32 | 6.69 | .007 | .28 | .01 | 77.38 | 15.24 | .06 | .17 | .07 | * | * |
| Inconel 718 | Huntington 52C9EK | .07 | .08 | 18.19 | .007 | .17 | .11 | 53.44 | 18.11 | .59 | 1.08 | .03 | 3.00 | 5.10 |

* Not determined

TABLE II

AVERAGE MECHANICAL PROPERTIES

| Material | Test Temp. | 0.2% Offset Yield Strength | Ultimate Strength | Uniform Elongation | Total Elongation | Reduction in Area | Number of Tests |
|---|---|---|---|---|---|---|---|
| Inconel 600* | 75°F<br>24°C | 35 ksi<br>241 MPa | 94 ksi<br>650 MPa | 33% | 39% | 67% | 2 |
| Inconel 600* | 800°F<br>427°C | 27 ksi<br>183 MPa | 86 ksi<br>590 MPa | 38% | 43% | 59% | 1 |
| Inconel 718** | 75°F<br>24°C | 148 ksi<br>1020 MPa | 191 ksi<br>1319 MPa | 18% | 19% | 32% | 4 |
| Inconel 718** | 800°F<br>427°C | 137 ksi<br>942 MPa | 167 ksi<br>1150 MPa | 15% | 18% | 29% | 3 |

* Strain Rate = $3 \times 10^{-4}$ $sec^{-1}$

** Strain Rate = $3 \times 10^{-5}$ $sec^{-1}$

TABLE III

IMPURITY LEVELS IN THE SODIUM (ppm)

| SPECIMEN NUMBER | MATERIAL | O* | H | C | Cl |
|---|---|---|---|---|---|
| 187 | Inconel 600 | 4.2 | 0.13 | 1.0 | 0.5 |
| 189 | Inconel 600 | 3.3 | 0.10 | <1.0 | <0.5 |
| 160 | Inconel 718 | 3.2 | 0.13 | <1.0 | ** |

* Almalgamation method results show total oxygen present: that tied up in stable compounds (e.g., metal oxides) as well as that present in a form which could interact with the crack tip.

** Not determined.

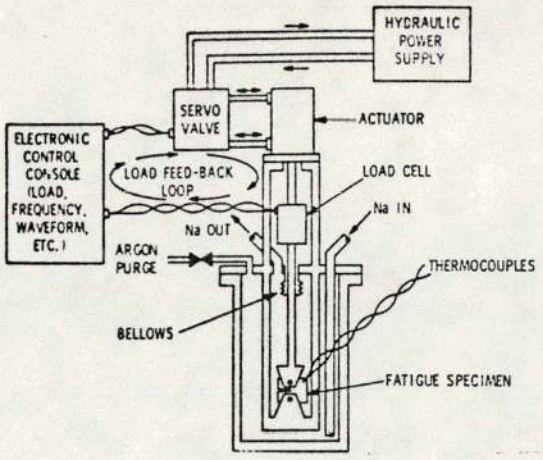


Figure 1. Schematic diagram of liquid sodium test chamber and loading system.

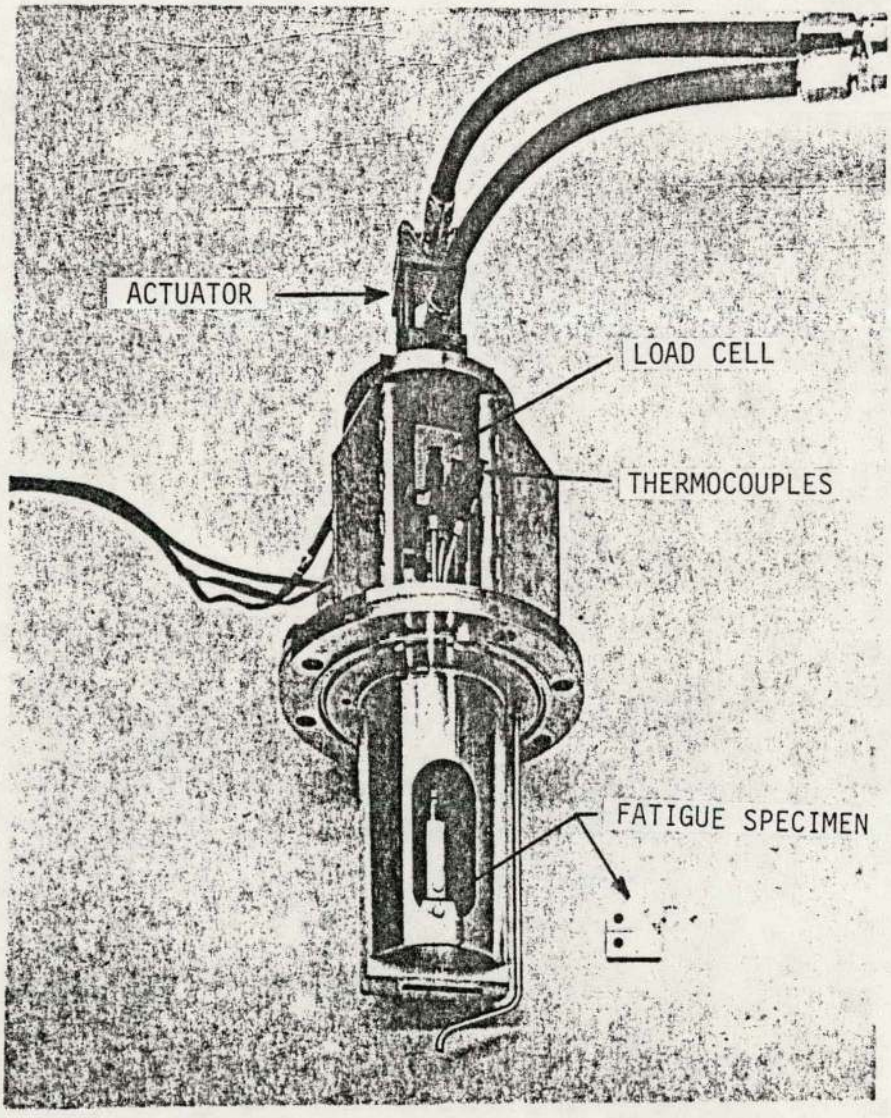


Figure 2. Liquid sodium fatigue loading system.

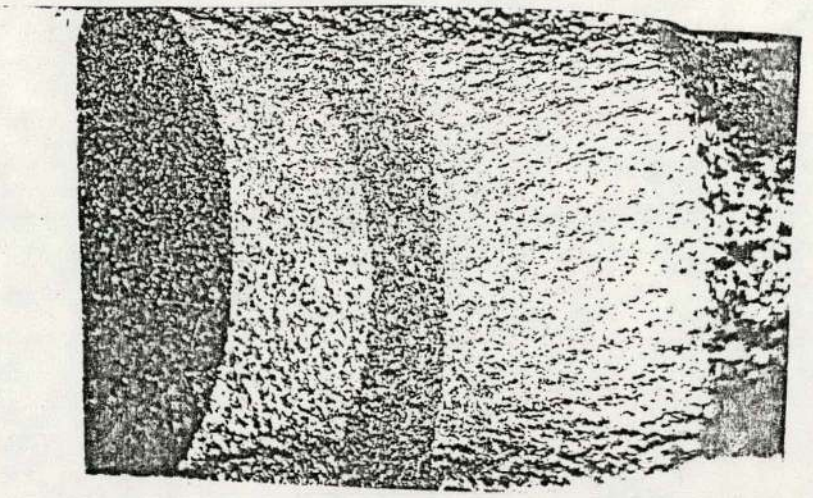

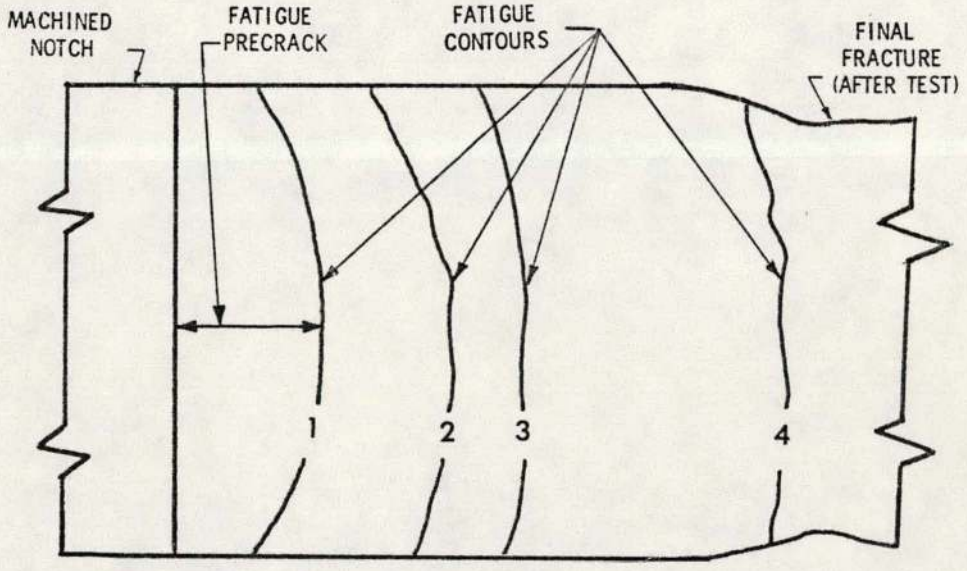


Figure 3. Fracture surface markings for Inconel 600 Specimen Number 187 tested in low-oxygen sodium at 800°F (427°C).

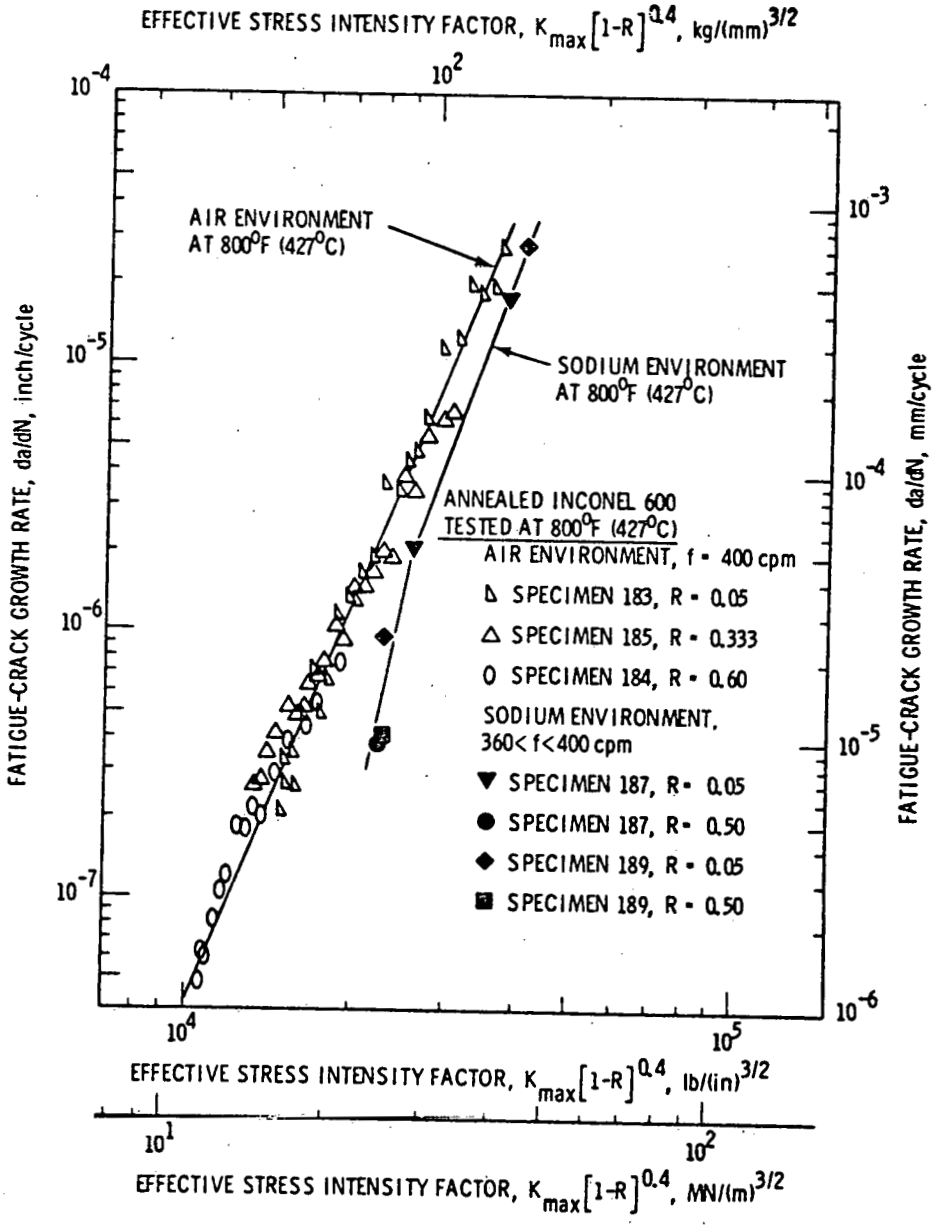


Figure 4. Fatigue crack propagation behavior of Inconel 600 in air and sodium environments at 800°F (427°C).

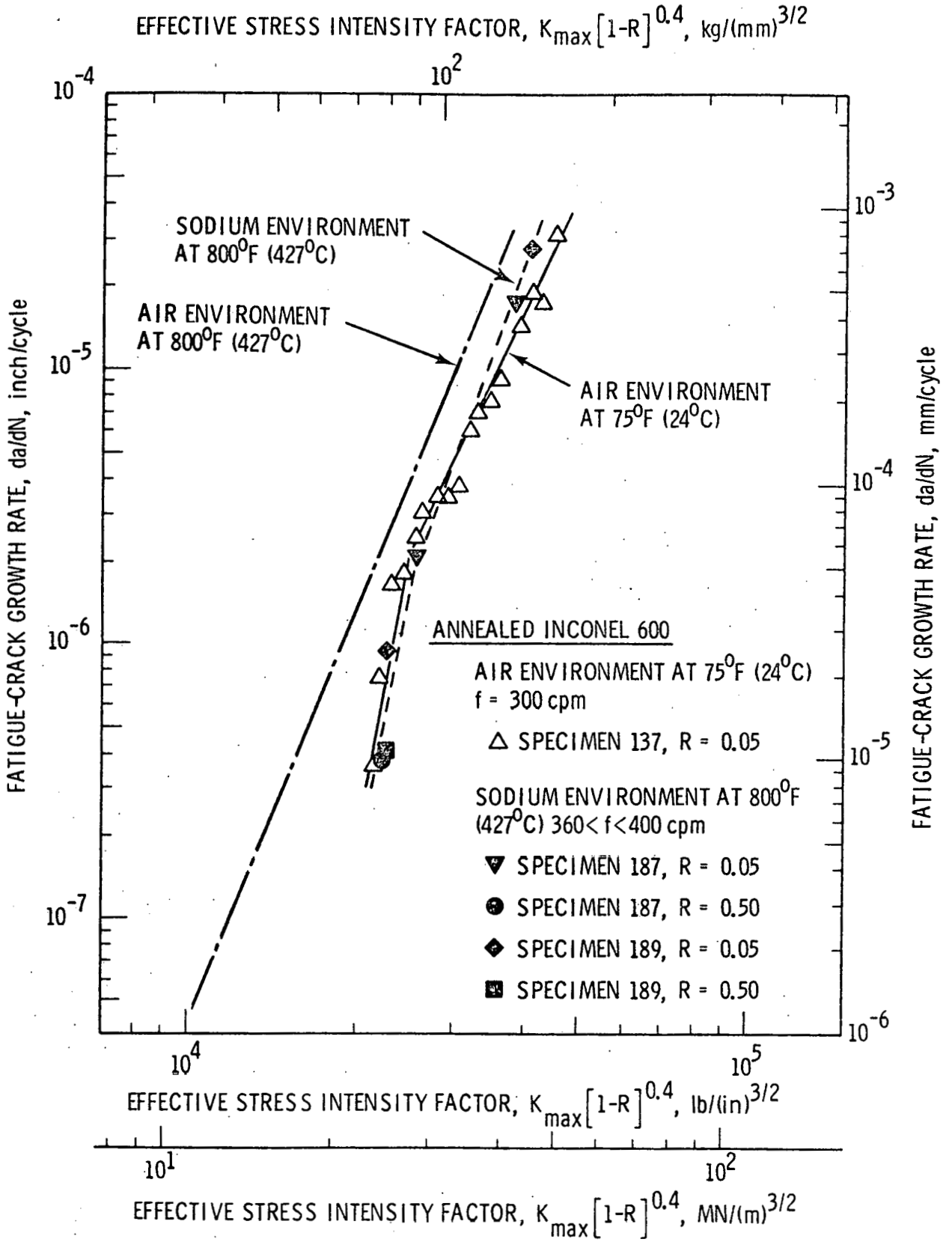


Figure 5. Fatigue crack propagation behavior of Inconel 600 in air and sodium environments at 800°F (427°C) and air at room temperature.

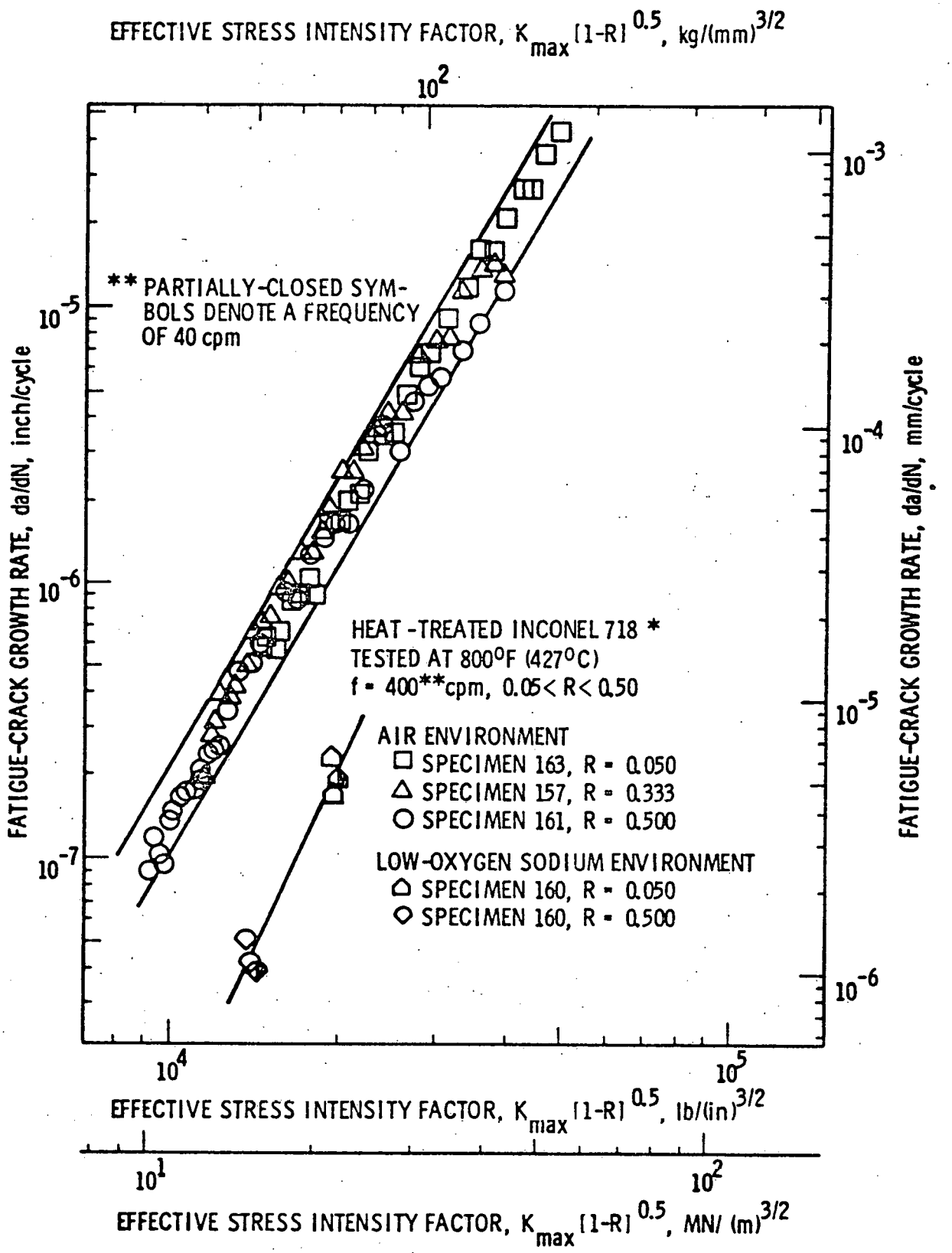


Figure 6. Fatigue crack propagation behavior of Inconel 718 in air and sodium environments at 800°F (427°C).

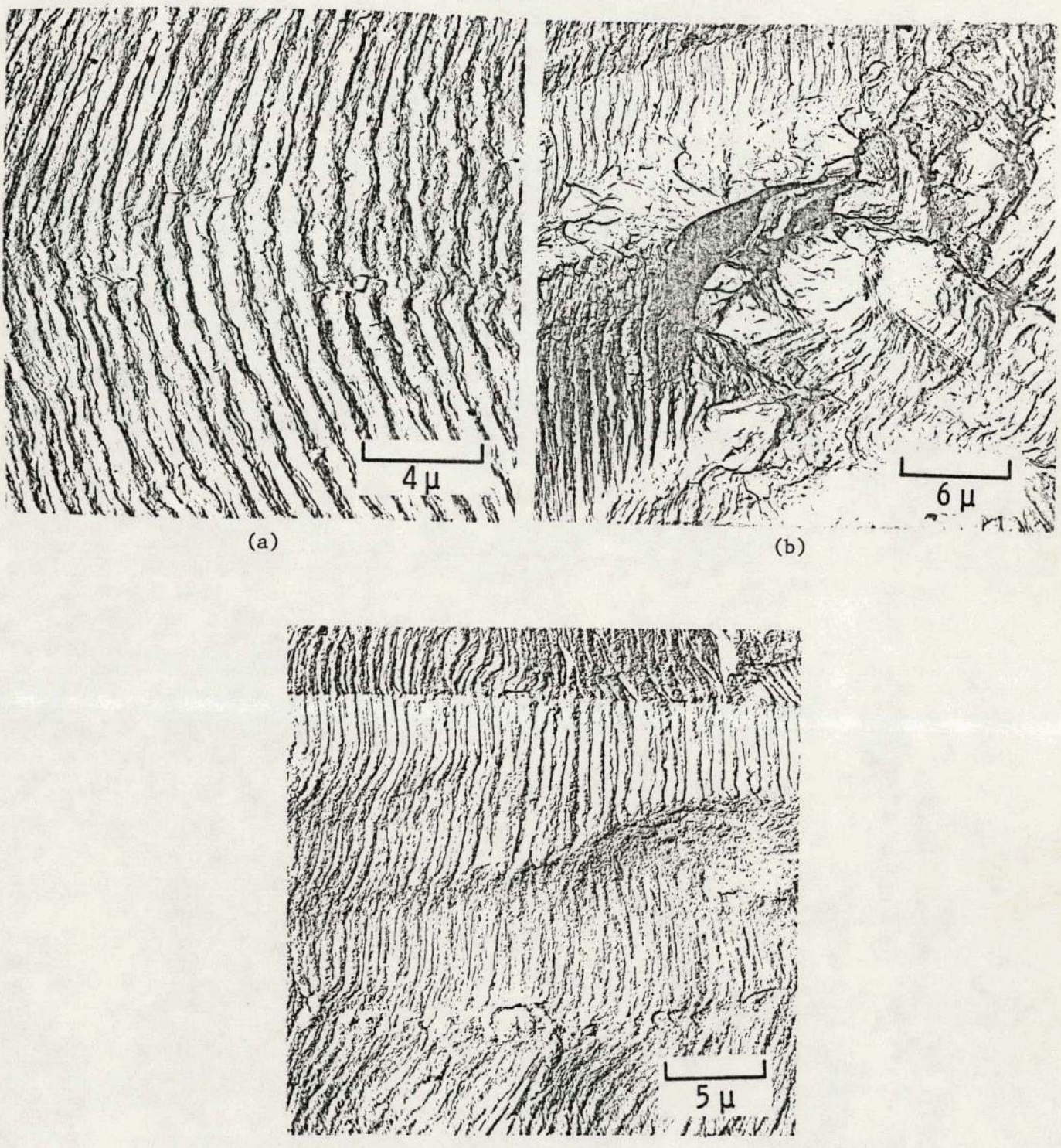


(a) (b)

(c)

Figure 7. Typical electron fractographs illustrating the 800°F (427°C) fatigue fracture surface micromorphology of Inconel 600 in air:

(a) well defined fatigue striations. [$K_{eff}$ = 40 ksi $\sqrt{in}$ (44 MPa $\sqrt{m}$)].
(b) fatigue striations coupled with microvoids. [$K_{eff}$ = 40 ksi $\sqrt{in}$ (44 MPa $\sqrt{m}$)].
(c) fatigue striations under intermediate stress intensity conditions. [$K_{eff}$ = 30 ksi $\sqrt{in}$ (33 MPa $\sqrt{m}$)].

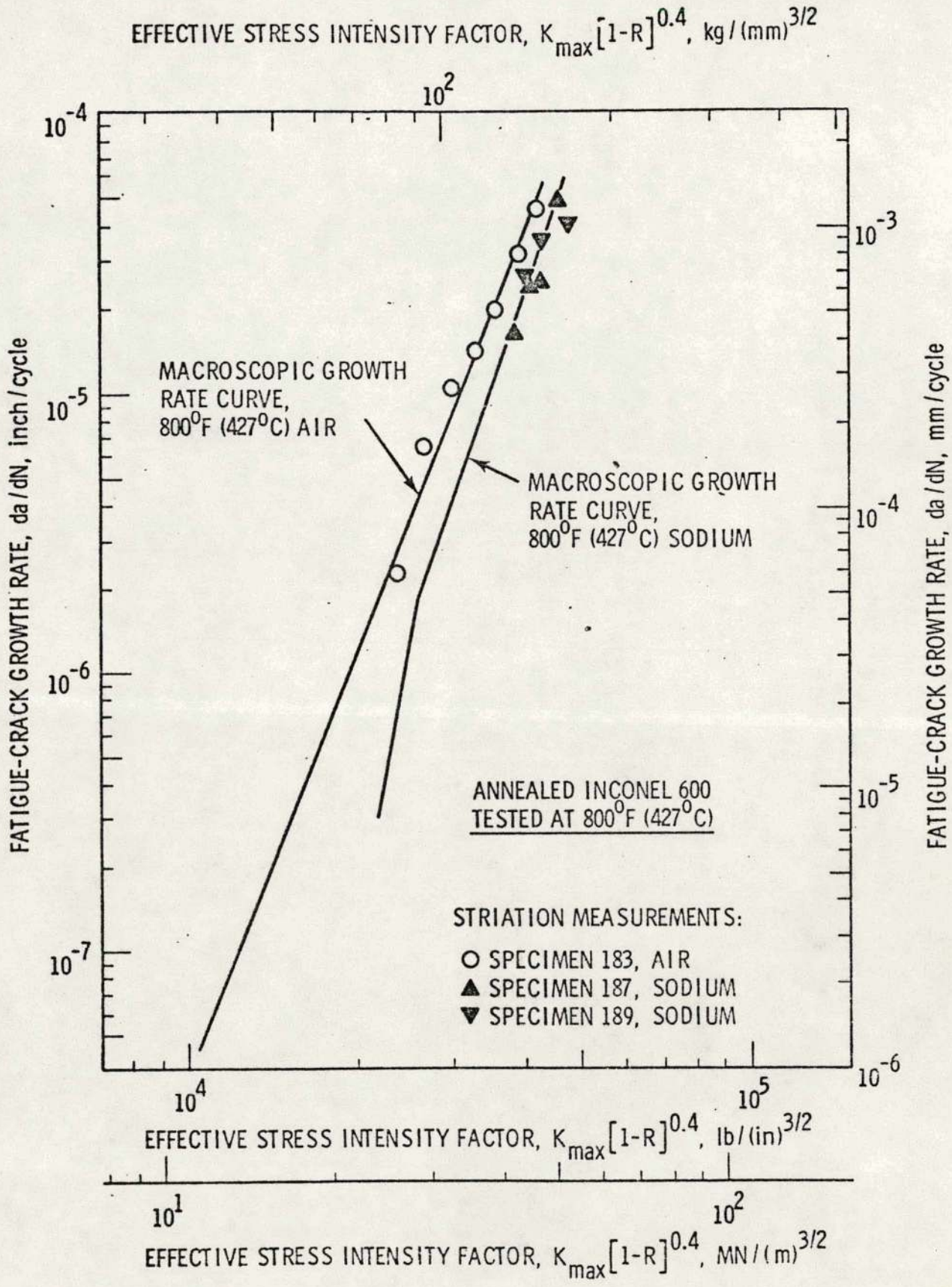


Figure 8 - Comparison of striation spacing measurements and macroscopic crack growth rates for Inconel 600 fatigue tested in air and liquid sodium at 800°F (427°C).

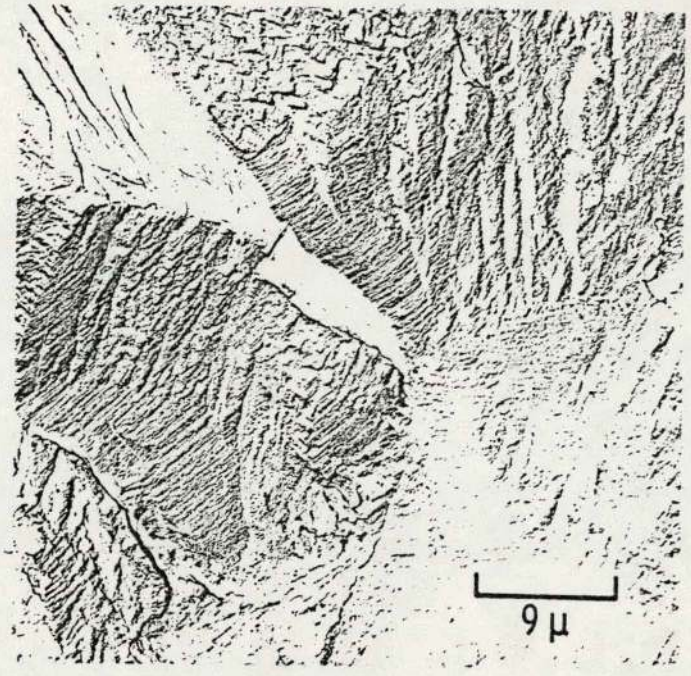


(a)

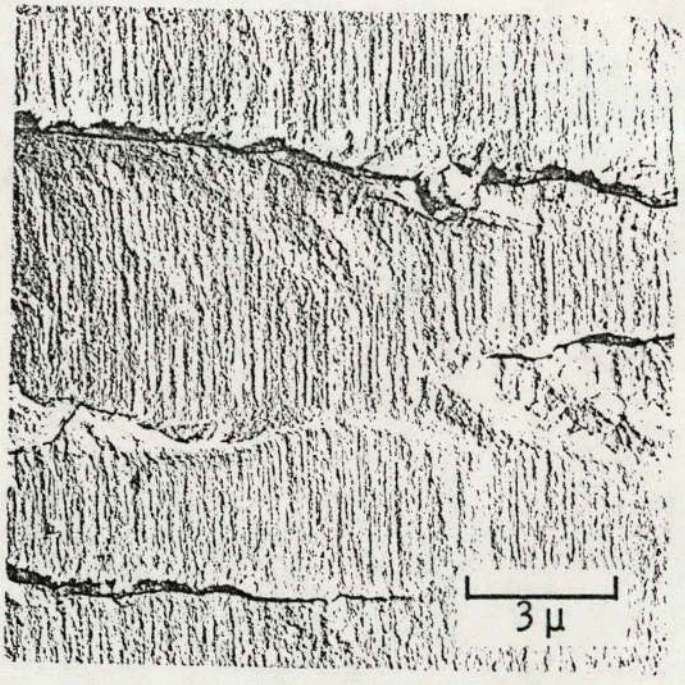


(b)

Figure 9. Electron fractographs revealing fatigue fracture surface micromorphology of Inconel 600 in air under low stress intensity factor conditions:

(a) cleavage-like faceted growth behavior with parallel fracture markings superimposed on facets. [$K_{eff}$ = 18 ksi$\sqrt{in}$ (20 MPa$\sqrt{m}$)].

(b) indistinct periodic fracture markings on crystallographic facets. [$K_{eff}$ = 20 ksi$\sqrt{in}$ (22 MPa$\sqrt{m}$)].

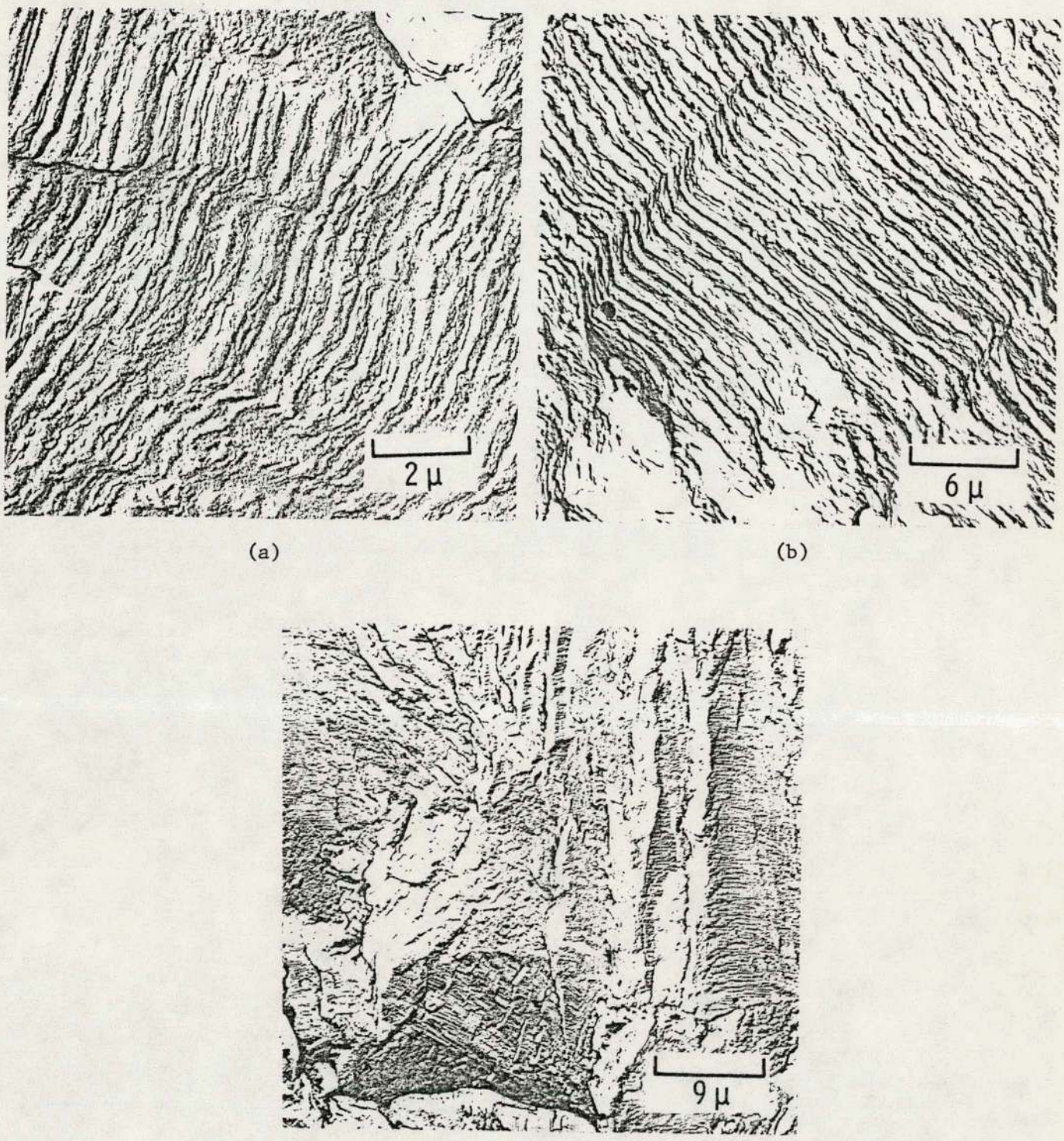


(a) (b)

(c)

Figure 10. Electron fractographs revealing the fatigue fracture surface appearance of Inconel 600 tested in liquid sodium at 800°F (427°C):

(a) fatigue striations observed at high stress intensity levels [Specimen No. 187; $K_{eff}$ = 44 ksi$\sqrt{in}$ (48 MPa$\sqrt{m}$)]
(b) fatigue striations observed at high stress intensity levels [Specimen No. 189, $K_{eff}$ = 44 ksi$\sqrt{in}$ (48 MPa$\sqrt{m}$)].
(c) faceted growth with periodic fracture markings superimposed on facets [Specimen No. 187; $K_{eff}$ = 22 ksi$\sqrt{in}$ (24 MPa$\sqrt{m}$)].

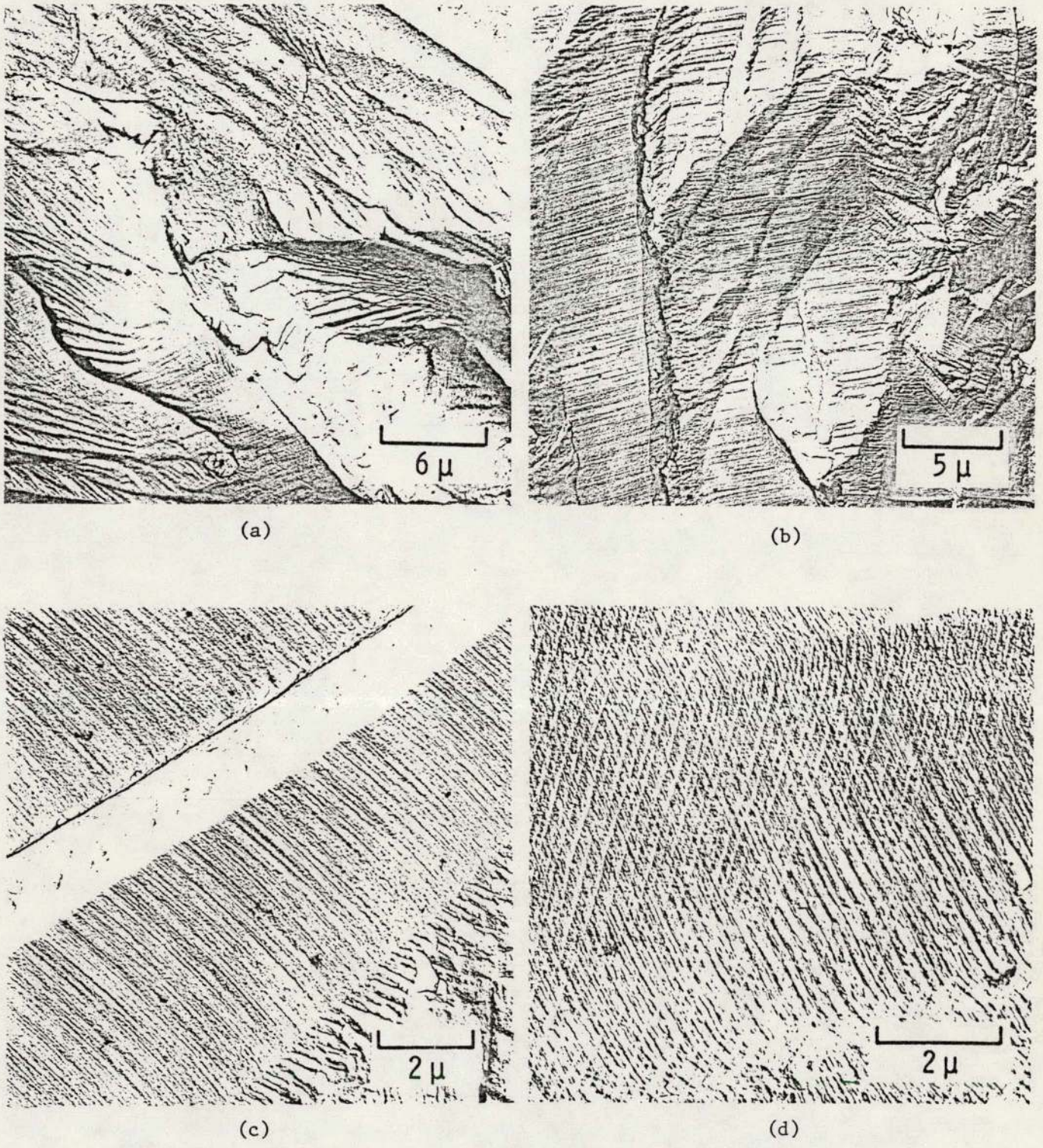


(a) (b)

(c) (d)

Figure 11. Typical electron fractographs of the Inconel 718 fatigue fracture surface in air under low $K_{eff}$ conditions:

(a) typical cleavage-like faceted growth.
(b) parallel fracture markings superimposed on cleavage-like facets.
(c) higher magnification of parallel fracture markings.
(d) two sets of parallel fracture markings.

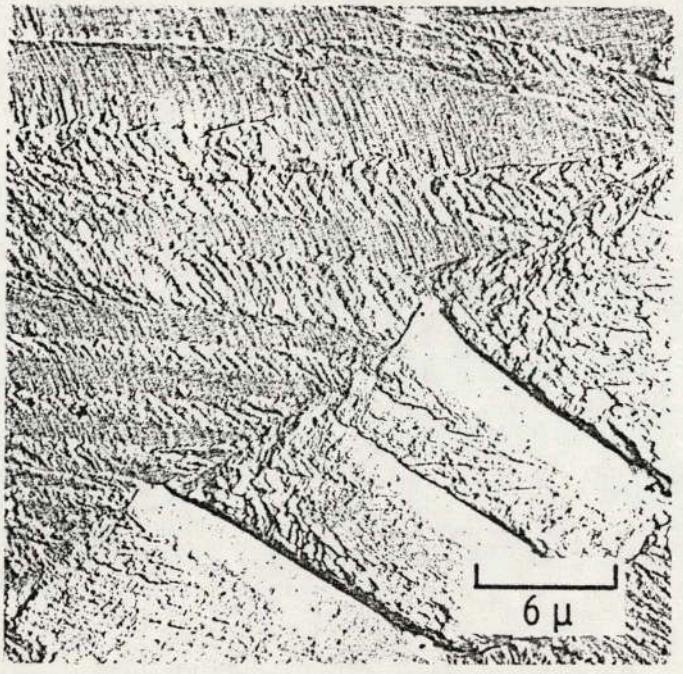


(a)

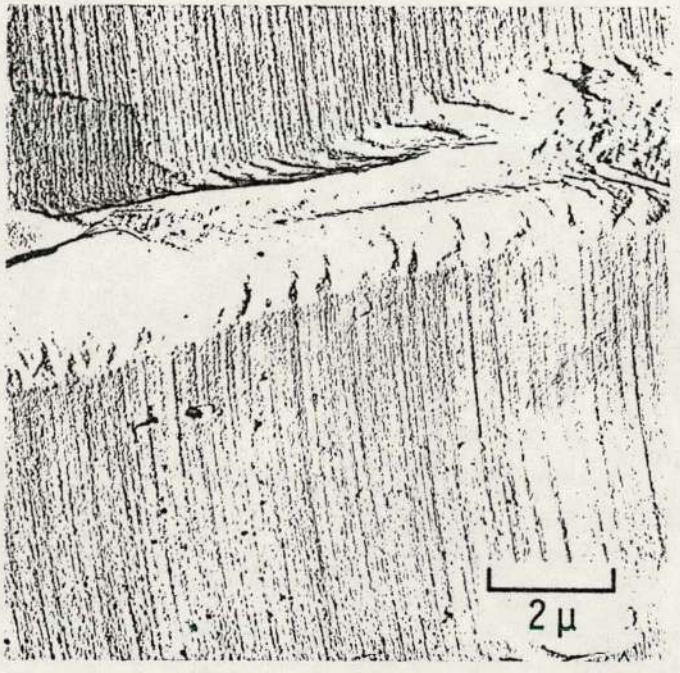


(b)

Figure 12. Typical electron fractographs illustrating Inconel 718 fatigue fracture surface in liquid sodium:

(a) typical faceted growth with periodic fracture lines superimposed.
(b) higher magnification of parallel fracture markings.